

A Novel Measurement Technique of Pure Out-of-Plane Vibrational Modes in Thin Films on a Nonmetallic Material with No Polarizer

Takeshi Hasegawa[†]

Kobe Pharmaceutical University, Motoyama-kita, Higashinada-ku, Kobe 658-8558, Japan

Received: October 9, 2001; In Final Form: February 1, 2002

A novel measurement technique has been developed to simultaneously obtain polarized spectra of in-plane (IP) and out-of-plane (OP) vibrational modes in optically thin films deposited on a nonmetallic substrate without using a polarizer. These spectra correspond to the conventional infrared transmission and reflection–absorption (RA) spectra, respectively. It has been commonly believed that the mode-selective measurements require polarizers and a specific surface. In particular, the OP-mode measurements always require a metallic surface to generate the surface-normal electric field in the films. The present technique overcomes the limitations of the measurements by considering the concept of virtual longitudinal-wave light using a new arithmetic regression model. The nonpolarized transmitted infrared ray through thin films on a transparent material (Ge) was collected at different angles of incidence, and the transmittance single-beam spectra were subjected to the chemometric spectral resolution, so that absorbance spectra were finally obtained. The two spectra resolved from the nonpolarization spectra were found to perfectly correspond to the conventional transmission and RA spectra. Since this technique is not affected by the enhancement factor that depends on a dielectric property of the metal surface, the band-intensity ratio of the two resolved spectra can be used for direct evaluation of molecular orientation in the films. Further, band shifts due to TO-LO splitting have clearly been observed on the nonmetallic substrate.

Introduction

Measurements of out-of-plane (OP) vibrational modes in thin films (molecular adsorbates) deposited on a nonmetallic substrate have been a crucial matter for condensed-matter physics^{1–3} and structural chemistry.^{4–6} Even when an infrared ray is irradiated on a film at a grazing angle, the surface-parallel component of electric vectors remains in the film due to an optical characteristic of nonmetallic substrates, which makes it impossible to *selectively* observe the OP vibrational modes only. The only way to prevent this problem is for the substrate to be metallic.^{7,8} In other words, no analytical technique has been available for the selective observation of in-plane (IP) and OP modes in films on an identical surface, since the observation of IP and OP modes requires infrared transparent and metallic substrates, respectively, and there is no material that satisfies both optical characteristics. Therefore, thus far, a film of interest has been deposited on infrared transparent and metallic substrates individually, which have been subjected to infrared transmission and reflection–absorption spectrometries, respectively. Nonetheless, this approach has the intrinsic disadvantage that the film needs contact with different materials, which often makes the films have a different structure depending on the different substrates. To overcome this dilemma, a new analytical technique for simultaneous observations of pure IP and OP modes on nonmetallic substrates has been urgently required for practical research and development.

For the simultaneous measurements, oblique-incidence transmission measurements through an infrared transparent material would be useful. When the substrate is highly transparent to the irradiated ray, however, the multiple reflections inside the

substrate produce optical fringes that make the reflection spectra complicated, and the optically complicated phenomena break the surface-selection rule of external-reflection spectroscopy.^{9,10} This is why selective measurements of the OP modes in films on transparent materials have not been realized thus far. Another experimental limitation is the impurity of polarization when polarizers are used.

If we had a specifically polarized beam of light whose electric vector is collinear with the wavenumber vector, the normal-incidence transmission measurements of the film would yield an ideal absorption spectrum of the OP modes. It is unfortunate, however, that such a longitudinal-wave light is not available in the *real* world as presented in the Maxwell equations. Nevertheless, if we consider the surface-normal component of electric fields of oblique-incidence infrared ray, the component would capture the OP modes. In other words, a perfect observation of OP modes could be achieved, if an arithmetic resolution of the surface-normal electric field from the total transmitted ray would be realized.

In the present study, the arithmetic resolution technique has been developed, and pure IP- and OP-mode infrared spectra of a 5-monolayer Langmuir–Blodgett (LB) film of cadmium stearate prepared on an infrared transparent plate (Ge) have readily been obtained from nonpolarized infrared oblique-angle transmission spectra. The analytical results suggested that this new technique not only yield the OP spectrum on a nonmetallic substrate but also allow molecular orientation to be directly analyzed with no knowledge of optical parameters. This approach has allowed a physically important problem about band shifts found between transmission and RA spectra, which has been unclear in the recent few decades, to be resolved.

[†] Corresponding author. E-mail: hasegawa@kobepharmaceutical-u.ac.jp. Fax: +81 78 435 2080.

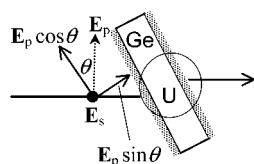


Figure 1. Schematic diagram of the observation of the LB film (dotted) deposited on a Ge plate at an angle of incidence of θ . The 0° polarization (\mathbf{E}_s ; thick circle) is perpendicular to the paper plane, while the 90° polarization (\mathbf{E}_p ; dotted arrow) is in the plane. The complicated optical phenomena after the irradiation are summarized by \mathbf{U} .

Material and Methods

A $40 \times 20 \times 2$ mm germanium substrate was purchased from Pier Optics (Gunma, Japan). The substrate was cleaned by a sonicator in pure water, ethanol, acetone, dichloromethane, and chloroform, successively, for 3 min each. For the chemicals and preparation method of the LB film, the reader is referred to a ref 5. The LB monolayers were deposited on both sides of the substrate. Since the LB film was subjected to transmission measurements, the infrared beam passed through the 10 layers in total.

The oblique-incidence infrared transmission measurements were performed by using a Brewster's Angle Sample Holder (BXH-S1G) by Harrick Scientific Co. (Ossining, NY). The angle of incidence was changed manually from 5° to 45° by a step of 5° . No polarizer was used for the measurements. The collection of infrared transmission spectra was performed on a Nicolet (Madison, WI) Nexus 670 FT-IR spectrometer equipped with a deuterated triglycine (DTGS) detector with a dry air flow in both the sample compartment and the spectrometer. The laser modulation frequency for the interferogram collection was 5 kHz. The interferogram was accumulated 300 times to improve the signal-to-noise ratio. The dry air was produced by an AirTech (Yokohama, Japan) AT-35H air drier.

The spectral collection was carried out so that "single-beam" (not absorbance) spectra were measured for both sample (LB/Ge/LB) and reference (Ge) measurements. The collected single-beam spectra that correspond to transmittance measurements with no apparatus correction were analyzed by a new chemometric-resolution equation, which will be discussed in detail in the next section.

Results and Discussion

Natural (nonpolarized) light comprises polarized beams with various directions. Therefore, the nonpolarization spectra capture information of both IP and OP modes. In other words, an unpolarized spectrum is a mixed spectrum of the IP and OP modes. The matter we have to address here is how to decompose the mixed spectrum into two pure spectra: \mathbf{s}_{IP} and \mathbf{s}_{OP} . To do that, a technique of classical least-squares (CLS) modeling^{11–13} has been employed, which is formulated by the following equation.

$$\mathbf{S} \cong \begin{pmatrix} \mathbf{s}_{\text{obs1}} \\ \mathbf{s}_{\text{obs2}} \\ \vdots \end{pmatrix} = \begin{pmatrix} r_{\text{IP1}} & r_{\text{OP1}} \\ r_{\text{IP2}} & r_{\text{OP2}} \\ \vdots & \vdots \end{pmatrix} \begin{pmatrix} \mathbf{s}_{\text{IP}} \\ \mathbf{s}_{\text{OP}} \end{pmatrix} + \mathbf{E} \cong \mathbf{R} \begin{pmatrix} \mathbf{s}_{\text{IP}} \\ \mathbf{s}_{\text{OP}} \end{pmatrix} + \mathbf{E} \quad (1)$$

Here, $\mathbf{s}_{\text{obs}j}$ is a row vector that represents an observed nonpolarized transmission (single-beam) spectrum at an angle of incidence, θ_j (Figure 1). The collection of $\mathbf{s}_{\text{obs}j}$ vectors by the variable-angle measurements forms the matrix, \mathbf{S} . This single-

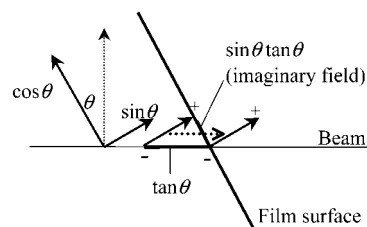


Figure 2. Scheme of the traveling of the $\sin \theta$ component. For the intuitive understanding of the imaginary electric field, sins of + and - are presented near the arrows.

beam spectra matrix can be theoretically represented by the pure IP- and OP-mode spectra, \mathbf{s}_{IP} and \mathbf{s}_{OP} , by use of mixing ratios in \mathbf{R} . For example, \mathbf{s}_{obs1} is a mixed spectrum of \mathbf{s}_{IP} and \mathbf{s}_{OP} with the mixing ratios of r_{IP1} and r_{OP1} ($\mathbf{s}_{\text{obs1}} = r_{\text{IP1}}\mathbf{s}_{\text{IP}} + r_{\text{OP1}}\mathbf{s}_{\text{OP}}$), which is a simple linear relation. The term \mathbf{E} represents an experimental error, noise and nonlinear factors, which do not obey the linear relation in terms of \mathbf{R} . The reason single-beam spectra are used for the modeling will be clarified later.

Therefore, if the \mathbf{R} matrix would be theoretically available, the IP- and OP-mode spectra would readily be deduced by the CLS regression:^{11–13}

$$\begin{pmatrix} \mathbf{s}_{\text{IP}} \\ \mathbf{s}_{\text{OP}} \end{pmatrix} = (\mathbf{R}^T \mathbf{R})^{-1} \mathbf{R}^T \mathbf{S} \quad (2)$$

This solution is often called a "compromised solution", which is mathematically equivalent to the least-squares solution.^{11–13} It is of note that the compromised solution by CLS regression extracts solutions that mostly satisfy the linear relationship defined by \mathbf{R} . In other words, nonlinear factors are automatically rejected in this regression calculation, and the rejected factors are pooled in the error term. Therefore, it is expected that highly pure spectra of IP and OP modes (\mathbf{s}_{IP} and \mathbf{s}_{OP}) will be extracted at this step.

Here, we have to confirm that a nonpolarized ray can be represented by only two orthogonal polarizations. The polarization-angle average of the nonpolarized ray is calculated as

$$2 \frac{\int_0^{\pi/2} (\cos \phi + i \sin \phi) d\phi}{\int_0^{\pi/2} d\phi} = \frac{4}{\pi} (1 + i) \quad (3)$$

in which ϕ is the angle of a specific linear polarization from the horizontal direction, and the real and imaginary parts represent the polarizations of 0° and 90° (\mathbf{E}_s and \mathbf{E}_p in Figure 1), respectively. This calculation clearly indicates that a nonpolarized ray can be represented by two perpendicular polarizations, but it requires a correction factor, $4/\pi$.

The polarized electric field of 0° (\mathbf{E}_s) is impervious to the angle of incidence (Figure 1), since it is always parallel to the film surface. Therefore, the 0° component detects the surface-parallel vibrational modes in the film regardless of the angle of incidence. On the other hand, the electric field of 90° (\mathbf{E}_p) has to be considered by two components: surface parallel ($\cos \theta$) and surface normal ($\sin \theta$). The $\cos \theta$ component travels along the light beam and interacts with the film surface collinearly (Figure 2) as does the 0° component, so that only the surface-parallel vibrational modes would be detected by the $\cos \theta$ component.

On the other hand, the $\sin \theta$ component is more complicated. When this electric-field vector travels with the beam (dotted arrow in Figure 2), the vector goes across the surface *obliquely*. Since an electric field plays a role of a microcondenser (denoted by + and - in Figure 2), this oblique travel of the microcon-

TABLE 1: Contribution of Electric-Field Components to the IP and OP Components, Generated from the Orthogonal Polarizations (E_s and E_p)

polarization relative intensity	E_s	E_p	
		$\sin \theta$	$\cos \theta$
IP	1	$\sin \theta \tan \theta$	$\cos \theta$
OP	0	$\tan \theta$	0

denser would produce a new surface-parallel electric field as well as the intrinsic surface-perpendicular component. Since the direction of travel is oblique, the interaction time of the surface-perpendicular component ($\sin \theta$) with the film is elongated by $1/\cos \theta$ to yield $\tan \theta$. The surface-parallel component is also evaluated in a similar way to be $\sin \theta \tan \theta$ by considering the geometry. Of note is that this electric field also interacts with the surface-parallel dipoles in the film. The contributions of the electric-vector components to IP and OP observations are summarized in Table 1.

Since the intensity of an electric vector is detected as a squared value, the \mathbf{R} matrix is finally obtained as

$$\mathbf{R} = \left(\frac{4}{\pi}\right)^2 \begin{pmatrix} 1 + \cos^2 \theta_j + \sin^2 \theta_j \tan^2 \theta_j & \tan^2 \theta_j \\ \cdot & \cdot \\ \cdot & \cdot \end{pmatrix} \quad (4)$$

This formulation is based on an assumption that all the electric fields do not interfere with each other, and the simple summation of the intensities is detected. After the infrared ray arrives at the surface, whose electric-field vectors obey the linear relation defined by \mathbf{R} , the transmitted ray in the film and substrate would experience complicated events, such as absorptions and multiple reflections. These unpredictable factors (represented by \mathbf{U} in Figure 1) are basically not modeled by the linear relation, and thus these factors would automatically be rejected by the regression calculation. Even if a portion of these rejected factors remains in s_{IP} and s_{OP} , it would be eliminated later by calculating the ratio of single-beam spectra of sample and reference. Therefore, single-beam spectra are necessarily collected, and subjected to the CLS resolution.

As a sample for our study, an LB film that consists of 5-monolayer cadmium stearate LB film deposited on both sides of a Ge plate was prepared, in which Ge is an infrared transparent material. Two sets of sample and reference single-beam spectra were collected at angles of incidence of 5° to 45° by 5° steps, and the sets were individually subjected to \mathbf{S} in eq 2 to yield new two sets of IP and OP single-beam spectra (s_{IP} and s_{OP} for sample and reference). The diagram of the procedures is presented in the Supporting Information. The OP single-beam spectrum is a virtual spectrum, as if an imaginary longitudinal-wave ray were normally irradiated on the film.

The IP and OP *absorbance* spectra have finally been calculated from the calculated single-beam spectra, which are presented in Figure 3. Of note is that almost identical results are obtained, even if a small number of spectra are used. For example, when two single-beam spectra measured at 30° and 15° are picked out and only seven spectra are subjected to the calculation, the analytical results are hardly changed. Instead, the range of angles of incidence is crucial. At least the range from nearly zero to 45° is necessary to adequately obtain information of both IP and OP components. The angle of incidence of 0° was considered to be experimentally risky, since the fine optical alignment error about 0° would largely influence the analytical result, and 5° was used for the smallest angle. Nevertheless, if very fine alignment were possible, an angle less than 5° would be chosen as the smallest angle.

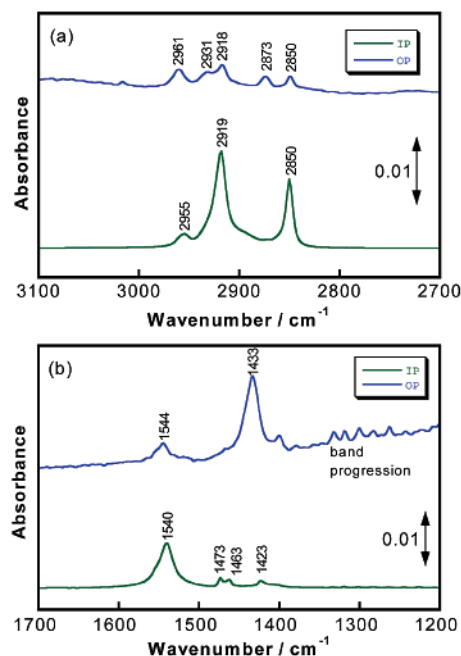


Figure 3. IP- and OP-mode spectra of the 5-monolayer cadmium stearate LB film on Ge resolved from the collections of nonpolarized spectra. The high and low wavenumber regions are separately presented in (a) and (b), respectively.

The antisymmetric and symmetric CH_2 stretching vibration bands ($\nu_a(\text{CH}_2)$ at 2919 cm^{-1} and $\nu_s(\text{CH}_2)$ at 2850 cm^{-1}), the CH_2 scissoring vibration bands ($\delta(\text{CH}_2)$ at 1463 and 1473 cm^{-1}), and the antisymmetric COO^- stretching vibration band ($\nu_a(\text{COO}^-)$ at 1540 cm^{-1}) appear strongly in the IP-mode spectrum, while these bands are suppressed in the OP-mode spectrum. When the cadmium stearate molecules stand on Ge perpendicularly, these bands have parallel transition moments to the film surface, which would result in the strong appearance in the IP-mode spectrum. In a similar fashion, the surface-normal transition moments, such as the symmetric COO^- stretching vibration band ($\nu_s(\text{COO}^-)$ at 1433 cm^{-1}) and band progression, appears strongly in the OP-mode spectrum. These facts indicate that the IP- and OP-mode spectra resolved by the new method truly correspond to the transmission spectrum on a transparent material and the reflection spectrum on a metal substrate, respectively. The pure OP spectrum measured on a nonmetallic substrate has never been reported.

This new analytical technique provides another physically interesting result. The IP and OP spectra in Figure 3b are found to exhibit different band positions (1423 and 1433 cm^{-1}) for an identical vibrational mode of $\nu_s(\text{COO}^-)$. This wavenumber shift for this band has already been found for infrared transmission and RA spectra, and two major hypotheses to explain the shift have been discussed thus far. One of them is that the shift is caused by a difference of chemical interaction between the monolayers and substrates.¹⁴ Since the transmission and RA techniques require two different substrates, the substrate surfaces can influence the monolayer structure through the chemical interaction. If the COO^- group interacts with a metallic surface more strongly than with an infrared transparent CaF_2 plate, for example, the band position in the RA spectrum would shift to a higher wavenumber than the transmission one.

The alternative hypothesis is that the shift is derived from a pure optical effect that is related to the longitudinal optic-transverse optic (TO-LO) splitting.¹⁴ Since LO modes can be coupled with a conservative electric field, the LO modes would selectively appear in the RA spectra,¹⁵ while TO modes

selectively appear in transmission spectra.¹⁴ In the infrared region, it is known that wavenumber shift obeys the Lydanne–Sachs–Teller (LST) rule.^{14,16} Nevertheless, the possibility of the chemical-interaction hypothesis has not yet been denied, since the mechanism of the TO-LO splitting in the noncrystal sample has been unclear, although some mechanisms have been proposed.^{14,17}

In the present study, however, the resolved results (IP and OP spectra) clearly deny the possibility of the chemical-interaction hypothesis. It should be noted that the $\nu_a(\text{COO}^-)$ and $\nu_s(\text{COO}^-)$ vibrational modes appear at 1544 and 1433 cm^{-1} in the OP spectrum, while they appear at 1540 and 1423 cm^{-1} in the IP spectrum. Since the analytical results are obtained from the identical sample, the shifts observed for the two modes cannot arise from the chemical interaction effect. Therefore, it is most possible that the splitting is caused by the TO-LO splitting. This conclusion suggests that both TO and LO modes are simultaneously observed by the oblique-incidence transmission measurements due to the optically thin film thickness.^{14–17} The shift is particularly clear for the $\nu_s(\text{COO}^-)$ band. The splitting of the $\nu_a(\text{COO}^-)$ vibration band has, thus far, been unclear due to the impurity of polarization. The present study, however, clearly indicates that there is a shift of 4 cm^{-1} . From a similar comparison, it has been confirmed that there is no difference between the IP and OP modes in the high wavenumber region (Figure 3a). The minor shift of the antisymmetric CH_2 stretching vibration (2917 and 2918 cm^{-1}) is believed to be a result of overlaying of the Fermi-resonance band that is found at 2931 cm^{-1} in the OP-mode spectrum.

Another benefit should also be emphasized that the new technique provides both IP and OP spectra with a common absorbance scale. Since both IP- and OP-mode spectra are obtained as if a polarized ray and an imaginary longitudinal-wave ray were respectively transmitted through the film perpendicularly, no enhancement factor need be considered, when a reflection measurement is performed on metallic substrates.¹⁸ In the present case, however, another important factor should be considered.

The nonpolarized light used in this study has two kinds of electric-field vectors on the film surface: IP and OP components. The IP component has two orthogonal directions of electric field, while the OP one has only one direction that is collinear with the light travel. When a transition moment in the film is considered with respect to the interaction with the electric fields, the moment would essentially interact with one electric-field vector, even if the two electric-field vectors of the IP component are irradiated. Since absorbance spectra are calculated by making the ratio of the total transmission intensity, however, the absorbance of the IP component would become half compared to that of the OP component. This means that we can directly compare the IP and OP band intensities by multiplying the IP component by a factor of 2 ($2I_{\text{IP}}$ and I_{OP}) for evaluation of the orientation angle (φ ; from the surface normal) of the mode

$$\varphi = \tan^{-1}(2I_{\text{IP}}/I_{\text{OP}}) \quad (5)$$

With this technique, the orientation angle of the $\nu_a(\text{CH}_2)$ and $\nu_s(\text{CH}_2)$ vibrational modes are calculated to be 84.1° and 85.2° from the surface normal, which gives the tilt angle of the hydrocarbon chain as 7.6°. In a previous work by Umemura et al., these angles were evaluated to be 85°, 85°, and 7°, respectively, by use of both transmission (on ZnSe) and RA (on silver) spectrometries. The present analytical result is very consistent with the previous results.¹⁸ In the same manner, the

orientation angles of the $\nu_a(\text{COO}^-)$ and $\nu_s(\text{COO}^-)$ vibration modes are calculated to be 78.3° and 7.7°, respectively. In the paper by Umemura et al. these angles were reported to be 83° and 18°, respectively. The discrepancy between the present work and the previous one would be due to the difference of the substrate, because the orientation of the COO^- group would strongly depend on the interaction of this group with the substrates. The previous technique always requires two different materials for substrates, and therefore it is not possible to directly compare the previous results to the present results. Regardless, the present results are considered to be acceptable and reliable, and it should be emphasized that the present results are evaluated by using no optical parameters. This implies that the new technique makes the molecular orientation analysis a relatively easy task.

Conclusion

The new analytical technique presented in this paper has been found to be a powerful means of measuring both IP and OP vibrational modes in optically thin films on infrared transparent materials. The analytical procedure could be made into an automatic routine, and the analysis of molecular orientation would be very easy for the user. Since this technique requires only one sample, we can prevent a problem that is caused by changing the substrate for the IP- and OP-mode measurements. Further, this technique would be applied to other regions of the electromagnetic spectrum used for the measurements.

Acknowledgment. This work is financially supported by Grant-in-Aid for Scientific Research on Priority Areas (A), “Dynamic Control of Strongly Correlated Soft Materials” (No. 413/13031074) from the Ministry of Education, Science, Sports, Culture, and Technology.

Supporting Information Available: Diagram of the present analytical procedures is available free of charge via the Internet at <http://pubs.acs.org>.

References and Notes

- (1) Berreman, D. W. *Phys. Rev.* **1963**, *130*, 2193.
- (2) Harbecke, B.; Heinz, B.; Grosse, P. *Appl. Phys.* **1985**, *A38*, 263.
- (3) Zhenjiang, C.; Madsen, J. M.; Takoudis, C. G. *J. Appl. Phys.* **2000**, *87*, 8181.
- (4) Yamamoto, K.; Ishida, H. *Appl. Spectrosc.* **1994**, *48*, 775.
- (5) Remizov, A. B. *J. Mol. Struct.* **1997**, *408/409*, 451.
- (6) Jones, L. H.; Swanson, B. I. *J. Phys. Chem.* **1991**, *95*, 2701.
- (7) Takenaka, T.; Umemura, J. In *Vibrational Spectra and Structure*; During, J. R., Ed.; Elsevier Science: Amsterdam, 1991; Vol. 19, p 215.
- (8) Hasegawa, T.; Kobayashi, Y.; Nishijo, J.; Umemura, J. *Vibr. Spectrosc.* **1999**, *19*, 199.
- (9) Hasegawa, T.; Takeda, S.; Kawaguchi, A.; Umemura, J. *Langmuir* **1995**, *11*, 1236.
- (10) Brunner, H.; Mayer, U.; Hoffmann, H. *Appl. Spectrosc.* **1997**, *51*, 209.
- (11) Kramer, R. *Chemometric Techniques for Quantitative Analysis*; Marcel Dekker: New York, 1998.
- (12) Beebe, K. R.; Pell, R. J.; Seasholtz, M. B. *Chemometrics: A Practical Guide*; Wiley-Interscience: New York, 1998.
- (13) Hasegawa, T. *Principle Component Regression and Partial Least Squares Modeling*. In *Handbook of Vibrational Spectroscopy*; Chalmers, John M., Griffiths, Peter R., Eds.; John Wiley: Chichester, U.K., 2002; Vol. 3, pp 2293–2312.
- (14) Yamamoto, K.; Ishida, H. *Vibr. Spectrosc.* **1994**, *8*, 1.
- (15) Kudo, K. *Hikaribussei-Kiso (Introduction to Optical Solid-State Physics)*; Ohmsha: Tokyo, 1996; p 69.
- (16) Ibach, H.; Luth, H. *Solid-State Physics: An Introduction to Principles of Materials Science*; Springer, New York, 1995.
- (17) Hasegawa, T.; Nishijo, J.; Umemura, J.; Theiss, W. *J. Phys. Chem. B* **2001**, *105*, 11178.
- (18) Umemura, J.; Kamata, T.; Kawai, T.; Takenaka, T. *J. Phys. Chem.* **1990**, *94*, 62.